Cellular and Molecular Bioengineering, Vol. 14, No. 6, December 2021 *(© 2021)* pp. 653–659
https://doi.org/10.1007/s12195-021-00690-z

Original Article

Permeability Properties of an *In Vitro* Model of the Alveolar Epithelium

VINOD SURESH [1,2,3]

[1]Auckland Bioengineering Institute, University of Auckland, Private Bag 92019, Auckland 1142, New Zealand; [2]Department of Engineering Science, University of Auckland, Private Bag 92019, Auckland 1142, New Zealand; and [3]Maurice Wilkins Centre for Molecular Biodiscovery, University of Auckland, Private Bag 92019, Auckland 1142, New Zealand

(Received 16 April 2021; accepted 7 July 2021; published online 21 July 2021)

Associate Editor Michael R. King oversaw the review of this article.

Abstract—Cell culture models of epithelial barriers in the body are widely used to study the permeation of nutrients, drugs, infectious agents and pollutants into the body tissues and circulation. The NCI-H441 cell line cultured at the air-liquid interface mimics certain phenotypic and functional characteristics of the human alveolar epithelium. Here the permeability properties of the NCI-H441 model were characterised and compared against published data using experimental measurements and mathematical modelling. Cells were cultured under air-liquid interface conditions and trans-epithelial electrical resistance (TEER) and apparent permeability (P_{app}) to sodium fluorescein (MW 383 Da) and fluorescently labelled dextrans (MW 4000–150,000 Da) was measured. It was found that TEER was independent of cell seeding density while P_{app} decreased with higher seeding density and plateaued beyond a density of 500,000 cells/cm^2. Using the framework of functional pore analysis, a mathematical model was fitted to P_{app} values measured in this work as well as previously published datasets from human cell lines and primary human and rat cells. It was found that the air-liquid interface NCI-H441 model most closely matched the primary cell line results in contrast to published data using A549 and liquid-interface NCI-H441 cell cultures, supporting the use of this model to study the permeability of the alveolar epithelium to large molecules.

Keywords—Pulmonary drug delivery, NCI-H441, Diffusion, Equivalent pore size, Paracellular.

INTRODUCTION

The respiratory surface of the human lungs in the alveoli is the largest surface of the body in direct contact with the external environment (approximately 100 m^2). Absorption across the thin epithelial lining of the alveoli permits entry of particulate matter, dissolved chemicals and microorganisms from the air space into the circulation. While inhaled drugs have traditionally been limited to local treatment of respiratory conditions, the respiratory epithelium is an attractive pathway for non-invasive systemic delivery since the large surface area and low enzyme activity in the lungs result in rapid absorption and increased bioavailability.[3] An increasing number of drugs are being assessed for delivery across the respiratory barrier. Cell culture models provide a relatively inexpensive and robust means for assessing the permeability of drugs across the respiratory epithelium. While cell culture models of the epithelial barrier in the trachea and bronchi are well characterised and widely used, models of the alveolar epithelial barrier are not as well developed.[4,5]

Previous studies have used human cell lines[13,20] and primary cells from rats[14] and humans[6] as *in vitro* models of the alveolar epithelial barrier. Inter-species differences in drug transporter identity and expression complicate the use of animal cells, while primary human cells are difficult to procure and maintain in the lab. Human cell line models thus offer a promising alternative. Commonly, the A549 and NCI-H441 cell lines have been used as models of the human alveolar epithelium. The NCI-H441 cell line cultured at an air-liquid has been shown to mimic the ion transport properties of *in vivo* human alveolar epithelium.[18] However, ion transport is primarily transcellular and mediated by transport proteins, while the paracellular pathway is important for the absorption of large, polar molecules.[9] Therefore, this study characterises the permeability properties of the air-liquid interface NCI-H441 model to paracellular tracers over a wide range of molecular masses. In order to effectively compare

Address correspondence to Vinod Suresh, Auckland Bioengineering Institute, University of Auckland, Private Bag 92019, Auckland 1142, New Zealand. Electronic mail: v.suresh@auckland.ac.nz

the results against existing literature, the mathematical framework of functional pore analysis is employed. The results indicate that the paracellular permeability of air-liquid interface NCI-H441 monolayers closely match that of primary cultures of human alveolar epithelial cells.

MATERIALS AND METHODS

Cell Culture

NCI-H441 cells (HTB-174) from the American Type Culture Collection (ATCC, USA) were used between passages 55 and 70. Cells were initially propagated in tissue culture treated flasks in propagation medium [RPMI-1640 (A10491-01, Life Technologies, New Zealand) supplemented with 10% fetal bovine serum (FBS)]. When the flasks were 70–80% confluent, cells were dissociated using Tryple reagent (Life Technologies, New Zealand) and seeded on clear Transwell inserts (Costar 3460, membrane area 1.12 cm^2, polyethylene terephthalate (PET) membrane, pore size 0.4 μm, thickness 10 μm, Corning, USA) at densities ranging from 2×10^4 to 2×10^6 cells/insert. Cells were cultured under submerged conditions with propagation medium in both the apical (0.5 mL) and basolateral (1.5 mL) chambers until confluence (typically overnight to 5 days) at which point cells were transferred to air-liquid culture by withdrawing liquid from the apical chamber The medium in the basolateral chamber was replaced with differentiation medium (RPMI-1640 supplemented with 4% FBS, 200 nM dexamethasone, 10 nM triiodothyronine (both from Sigma Aldrich, New Zealand) and 1% insulin-selenium-transferrin solution (Life Technologies, New Zealand)) to promote the formation of a polarised epithelium (typically 7–10 days). Culture medium was changed every 2 days. Transepithelial electrical resistance (TEER) and potential difference (TEPD) were measured using a voltohmmeter (Endohm-12, World Precision Instruments, Australia) at each medium change to monitor cell health and polarisation status.

Transport Experiments

Transport measurements were carried out when the TEER was greater than 250 Ω cm^2 and remained stable over 3 days. Culture medium was removed and both chambers rinsed gently with warm Hanks Balanced salt Solution (HBSS, catalogue number 14025092, Life Technologies, New Zealand). HBSS was then added to the apical (0.5 mL) and basolateral (1.5 mL) chambers and cells were allowed to equilibrate for 30 min. Then 10 μL of sodium fluorescein (Sigma Aldrich, New Zealand) or fluorescein isothiocyanate (FITC) conjugated dextrans (molecular masses 4, 10, 40, 70, 150 kDa, all from Sigma Aldrich, New Zealand; corresponding molecular radii 14, 23, 45, 65, 85 Angstrom) were added to the donor (apical) chamber to a final concentration of 10 μM. Buffer from the acceptor (basolateral) chamber was sampled (100 μL) was sampled at regular intervals for 2 h. After each sampling fresh HBSS was added to the basolateral chamber to maintain the volume constant. All measurements were carried out at 37 °C. Samples were stored at 4 °C and analysed the same day to determine the concentrations of the fluorescent tracers using an EnSpire MultiMode plate reader (PerkinElmer, USA).

Data Analysis

For a purely paracellular tracer diffusing from a donor chamber (concentration C_0) to an acceptor chamber (volume V, concentration C) under sink conditions ($C_0 \gg C$), the transport rate is given by

$$V\frac{dC}{dt} = P_{app}A_m C_0, \tag{1}$$

where P_{app} is the apparent permeability and A_m is the membrane area. This equation was used to determine the apparent permeability for each of the tracers from the slope of the concentration vs. time plot. The validity of the transport model was verified by checking that the concentration in the acceptor chamber increased linearly with time and that sink conditions were met.

Functional Pore Size Analysis

Following,[22] the paracellular pathway was considered to consist of two populations of straight, cylindrical pores with different radii. Diffusion of tracers in the smaller pores is restricted while free diffusion conditions exist in the larger pores. The restrictive population consists of n_s straight cylindrical pores with radius r_s and length l_s. The effective diffusion coefficient D_{eff} for a solute of molecular radius r diffusing through one such pore is:

$$D_{eff} = D_\infty\left(1 - \frac{r}{r_s}\right)^2, \tag{2}$$

where D_∞ is the free diffusion coefficient in an unbounded medium and is given by the Stokes–Einstein relation:

$$D_\infty = \frac{k_B T}{6\pi\mu r}, \tag{3}$$

where k_B is Boltzmann's constant, T is the absolute temperature and μ is the dynamic viscosity of the medium. The factor $\left(1 - {}^{r}/_{r_s}\right)^2$ in Eq. (2) accounts for steric exclusion of the solute from the region in the vicinity of the pore wall. Under the assumption of sink conditions, the rate of diffusive transport Q_s of solutes through this population can be written using Fick's first law as:

$$Q_s = (n_s) \times (\pi r_s^2) \times \left(D_{\text{eff}} \frac{dc}{dx}\right) \sim \frac{k_B T n_s}{6\mu} \frac{r_s^2}{r} D_\infty \left(1 - \frac{r}{r_s}\right)^2 \frac{C_0}{l_s}. \quad (4)$$

Similarly the rate of free diffusive transport though the population of n_l large pores of radius r_l and length l_l is equal to:

$$Q_l \sim \frac{k_B T n_l r_l^2}{6\mu r} D_\infty \frac{C_0}{l_l}. \quad (5)$$

By equating the total rate of transport ($Q_s + Q_l$) to Eq. (1), the following relationship is obtained between the apparent permeability and pore geometry:

$$P_{\text{app}} = \alpha \frac{r_s^2}{r} \left(1 - \frac{r}{r_s}\right)^2 + \frac{\beta}{r}, \quad (6)$$

where α and β are parameters related to the pore geometry and number and are given by:

$$\alpha = \frac{k_B T n_s}{6\mu l_s A_m}, \beta = \frac{k_B T n_l r_l^2}{6\mu l_l A_m}. \quad (7)$$

Equation (6) was fitted to P_{app} values measured over a range of solute radii r to determine r_s, α and β using the constrained nonlinear optimisation function *fmincon* in the global search mode (Matlab v2015b, Mathworks Inc, Cambridge MA).

RESULTS

Effect of Cell Density on Layer Properties

Four seeding densities (20,000; 100,000; 500,000; 2,000,000 cells/insert) were used to assess the effect of cell density on barrier properties. At the two lowest densities cells required 5 and 3 days respectively of submerged culture to reach confluence (visually assessed on a microscope). Cells seeded at higher densities formed confluent layers overnight. Cells were then maintained under air-liquid culture conditions and barrier development was monitored by measuring TEER every 2 days. TEER exhibited a linear increase over 8 days after establishing air-liquid culture to a maximum value of 300–400 Ω cm^2 and values remained fairly stable and larger than 250 Ω cm^2 for a further 12 days (Fig. 1a). In general, higher seeding densities corresponded to higher TEER, but the difference was not statistically significant. There was also no significant effect on the time required to reach maximum TEER. Since TEER is a measure of the permeability of the cell layer to small inorganic ions (primarily sodium and chloride) the results suggest that cell density does not have a significant effect on the transport of these ions.

Next, the apparent permeability P_{app} of the cultures to the paracellular tracer sodium fluorescein was measured. It was found to correlate negatively with cell density (Spearman's $\rho = -0.92$) and decreased almost ten-fold between the lowest and highest seeding densities (Fig. 1b). Pairwise comparison using the Tukey range test indicated significant differences ($P < 10^{-4}$) between each pair except the two highest seeding densities. In measurements with cell free inserts there was rapid permeation of sodium fluorescein from the apical to basolateral chambers, indicating that the diffusion resistance of PET membrane is negligible (data not shown).

Taken together the TEER and P_{app} measurements indicate that ion transport is unaffected, but permeability to paracellular tracers decreases as seeding density is increased and reaches a plateau at a density of 500,000 cells/insert. This seeding density was used for subsequent experiments.

Permeability of Dextrans

The concentration of fluorescently labelled dextrans in the basolateral chamber increased linearly with time (Fig. 2a). The maximum concentration in the basolateral chamber was less than 0.1% of the concentration in the apical chamber indicating that sink conditions were met. Values of the apparent permeability P_{app} determined from these measurements are listed in Fig. 2b. Apparent permeability decreased with molecular mass m. A power law relationship fitted the data well ($P_{\text{app}} \sim 3 \times 10^{-5} m^{-0.78}$, Fig. 2c), suggesting that the transport of dextrans across the cell layer reflects hindered diffusion through a porous medium.[1]

Pore Size Analysis

Figure 3a shows the results of fitting the theoretical model (Eq. 6) to the data. For comparison, four other data sets extracted from the literature are plotted. The model fits the data well. Estimates of the model parameters for all data sets are shown in Table 1. Parameter estimates from our data match closely with estimates derived from primary cultures of rat[14] and

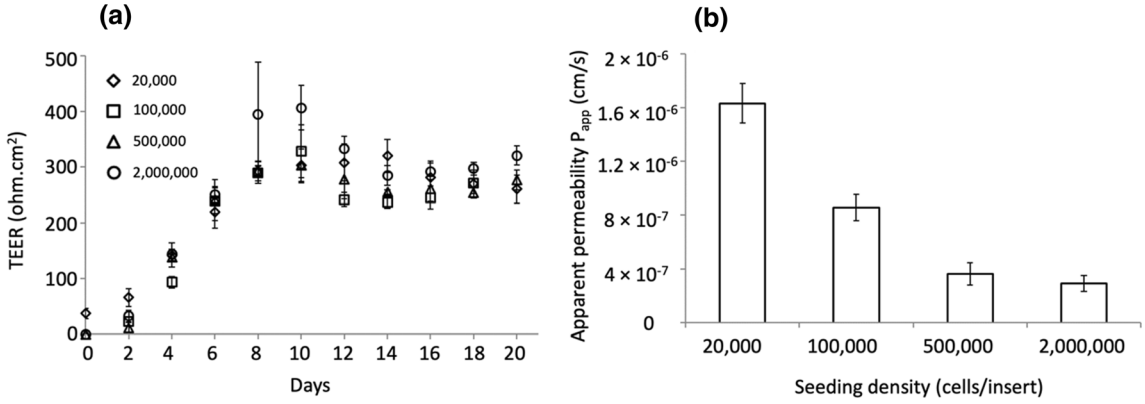

FIGURE 1. Epithelial barrier function assessed by trans-epithelial electrical resistance (TEER) and apparent permeability P_{app} to a paracellular tracer show different characteristics. (a) A functional epithelial barrier develops in 8–10 days following cell seeding and exposure to air-liquid interface indicated by the increase in TEER; the barrier remains stable over a period of about 10 days indicated by the plateau in the TEER values. (b) While the TEER is insensitive to the cell seeding density, P_{app} shows a significant decreasing trend as the seeding density increases. Data points represent mean ± SD (n = 6).

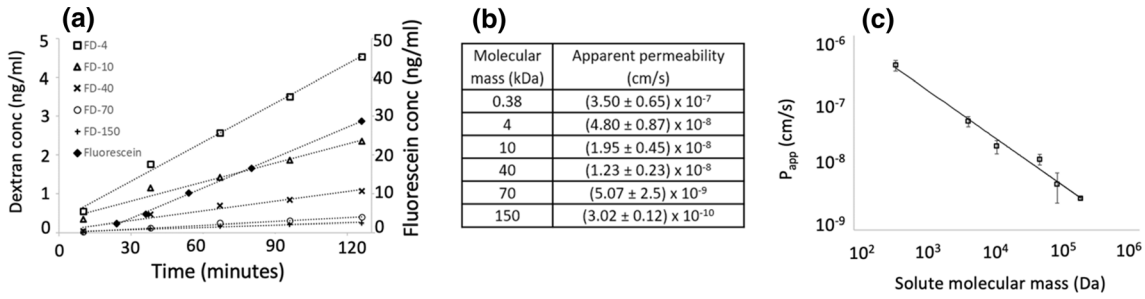

Molecular mass (kDa)	Apparent permeability (cm/s)
0.38	(3.50 ± 0.65) x 10^{-7}
4	(4.80 ± 0.87) x 10^{-8}
10	(1.95 ± 0.45) x 10^{-8}
40	(1.23 ± 0.23) x 10^{-8}
70	(5.07 ± 2.5) x 10^{-9}
150	(3.02 ± 0.12) x 10^{-10}

FIGURE 2. Transport of dextrans across NCI-H441 cell layers is consistent with passive diffusion. (a) The concentration of the tracer species increases linearly with time. Symbols represent measurements and dotted lines represent linear best fits (left axis for FITC-conjugated dextrans (FD), right axis for sodium fluorescein). (b) P_{app} values over a range of solute molecular masses (mean ± SD, n = 6). (c) The apparent permeabilities P_{app} (symbols) calculated from the data show a power law relationship (dotted line) with the molecular mass of the solute, characteristic of hindered diffusion through a porous material.

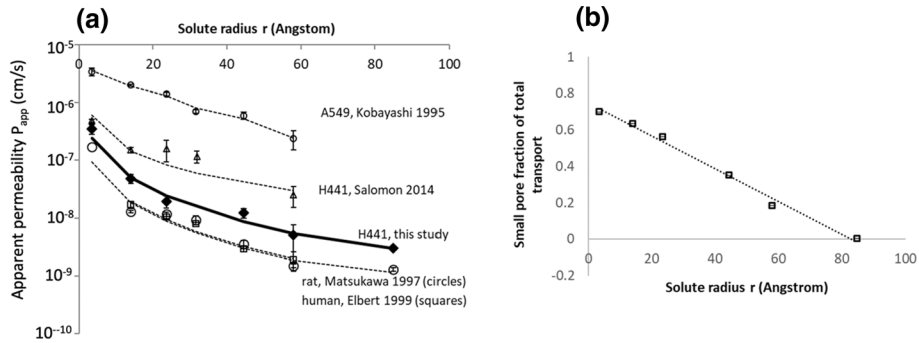

FIGURE 3. Permeability profile across NCI-H441 cell layers is consistent with the two-pore population model. (a) A semi-log plot of P_{app} against the solute radius show good agreement between the data (filled diamonds) and model (heavy solid line) for this study with root mean square deviation (RMSD) of 0.20. Other datasets extracted from the literature (open symbols) and the corresponding model fits (dotted lines) are plotted for comparison. RMSD values for these fits range from 0.08 to 0.34. (b) The fraction of the total flux passing through the small pore population is plotted as a function of the solute radius. Open squares indicate data points and the dotted line is the linear best fit.

human[6] alveolar epithelial cells. In contrast, estimates from A549[13] and liquid-interface NCI-H441[20] models were qualitatively different in that they suggested a single pore population. We comment further upon this observation in the discussion. In addition, the pore size estimated from the measurements is about 50 times smaller than the pore size of the PET membrane on which the cells are grown, confirming that the measurements primarily characterise the cell layer and the

TABLE 1. Parameter values determined by fitting Eq. (6) to measurements (this study) and historical data extracted from the literature.

Parameter	This study	Salomon 2014 (NCI-H441)	Elbert 1999 (human)	Matsukawa 1997 (rat)	Kobayashi 1995 (A549)
r_s (nm)	8.26	59.3	7.14	7.19	21.59
$\alpha(\times 10^3/s)$	9.38	0.60	5.05	4.81	122
$\beta(\times 10^{15} cm^2/s)$	2.54	–	1.06	0.97	–

contribution of the membrane to transport resistance is small.

Figure 3b shows the fraction of the total transport carried through the small pores, i.e. $Q_s/(Q_s + Q_l)$. Even for the small solute (fluorescein), only about 70% of the total transport is carried through the small pore population and roughly 30% passes through the large pores. This fraction increases almost linearly with the molecular radius of the solute.

DISCUSSION

Cell culture models of the alveolar epithelium are a useful tool for drug screening and permeability studies. Generally, the use of primary alveolar epithelial cells has been recommended,[12,19] however the difficulty of access to and maintenance of primary cells by long term passaging poses an obstacle to their use. The focus of this work was to investigate the potential of NCI-H441 cells cultured at an air liquid interface as an *in vitro* model for paracellular permeation across the human alveolar epithelium. The results indicate that this *in vitro* model closely matches primary alveolar epithelial cell culture models from humans and rats.

The NCI-H441 cell line was established from a human subject with papillary adenocarcinoma and have been demonstrated to exhibit phenotypic and functional characteristics of alveolar epithelial cells.[5,18] They have also been shown to have drug transporter expression profile similar to primary cultures of human alveolar epithelial cells when cultured under liquid submerged conditions.[20] In Ref. 20, permeability measurements were not carried out under air-liquid interface conditions that are representative of the *in vivo* condition and commonly used in primary cell culture models.[6,14]

Typically, the trans-epithelial electrical resistance (TEER) is used as a measure of the barrier functionality of epithelial cell cultures. Depending on the cell type and culture conditions, TEER values range from less than 100 Ω cm^2 to more than 1000 Ω cm^2. The TEER primarily reflects the permeability of the cell layer to sodium and chloride ions *via* transcellular as well as paracellular pathways and thus is not a perfect proxy for the permeability to cell impermeable paracellular tracer molecules. Consistent with this idea, it was found that the peak TEER and the time to peak TEER was independent of the cell seeding density, while P_{app} decreased with seeding density (Fig. 1).

In order to provide an objective comparison between different models, published permeability data[6,13,14,20] were reanalysed by fitting a mathematical model of passive solute permeation to the measurements.[22] This approach partitions the permeation pathway into two components, one through a population of small pores and the second through a population of larger pores. Solutes that are larger than the radius of the small pores permeate exclusively through the second pathway, while smaller solutes can move through both pathways. The analysis shows that air-liquid interface NCI-H441 cells and primary alveolar epithelial cells exhibit very similar permeation properties (Table 1) with a small pore radius (r_s) of 7–8 nm. The parameters α and β are roughly twice as large as the values for the primary cultures and may be interpreted as an increase in the overall number of pores in the NCI-H441 model. In contrast, the data for A549[13] and liquid-submerged NCI-H441[20] cells are consistent with a single pore population with a much larger value for r_s; consequently there is no equivalent large pore population (i.e. the parameter β is undetermined).

While this work and the studies compared in Fig. 3a[6,13,14,20] all use tissue culture (Transwell) inserts, a number microfluidic devices (“lung-on-a-chip”) of varied designs have been developed as *in vitro* models of the alveolar barrier.[8,11,15,21,23] These devices have used various cell types, including A549,[8,15] NCI-H441[11] and primary human cells.[21,23] Permeability measurements in these studies have utilised a limited set of paracellular tracers. The apparent permeability of FITC sodium (similar molecular weight to sodium fluorescein) measured in these studies varied across one order of magnitude (0.15×10^{-6} cm/s,[15] 0.65×10^{-6} cm/s,[21] 9×10^{-6} cm/s[23] 15×10^{-6} cm/s[8]); for comparison the current work found a value of (0.35 ± 0.065) $\times 10^{-6}$ cm/s. Stretch and shear flow were found to have a significant effect on permeability: shear flow was found to reduce the apparent permeability of FITC sodium from 15×10^{-6} to 6×10^{-6} cm/s[8] while cyclic stretch was found to increase the apparent per-

meability from 0.65×10^{-6} to 4.5×10^{-6} cm/s.[21] Microfluidic devices can recreate more realistic physiology in their small dimensions and the ability to provide stretch and fluid flow, and also the potential of high throughput studies along with reduced use of consumables. However, device designs, materials, fabrication protocols and experimental protocols are at present customised by each research group in contrast to tissue culture inserts that are available off-the-shelf from commercial suppliers and for which standardised protocols have been adopted.

This study focused on the transport of cell impermeable tracer molecules in the size range 400–150,000 Da. This range encompasses the size of therapeutic molecules considered for systemic delivery across the pulmonary epithelium, though the most common size range is 1000–10,000 Da.[17] It should be noted that the effective molecular masses are likely to be larger since drug molecules will typically be conjugated to carrier compounds in order to promote delivery, absorption and bioavailability.[2] The results from this study can provide an initial estimate of permeation rates for a given molecular mass and a specific *in vitro* model. When testing the permeation of a therapeutic molecule, including a panel of paracellular tracers bracketing its molecular size will help assess if the transport of the therapeutic molecule fits the profile of paracellular absorption.

The equivalent pore sizes determined in this study are based upon a purely functional analysis. In reality, paracellular pores have a physical existence in tight junctions that connect adjacent cells and their structure is determined by the presence of and interactions between a number of junctional proteins.[10,24] The claudin family of proteins (26 of which are found in humans[10]) are particularly important in determining paracellular permeability. Of these, the most highly expressed in alveolar epithelial cells are claudins-3, 4, 5, 7 and 18.1.[7,10,16] The relationship between claudin expression and paracellular permeability is complex: different claudins form the structural elements of seals (claudins 3, 4, 5 in alveolar epithelium) or pores (claudin 7 in alveolar epithelium) that are charge selective.[10,24] Claudin-4 has been found to have a protective role in acute lung injury by promoting barrier formation and fluid clearance,[7] while the expression of other alveolar epithelial claudins have been found to be altered in various lung pathologies such as alcoholic lung syndrome and pulmonary fibrosis.[16] We have previously detected gene and protein expression of claudins-3, 4, 5 in NCI-H441 cultures.[18] While the importance of claudins in regulating the paracellular permeability of small ions is well established, their role in the permeability of large macromolecules such as the dextrans used here is not fully understood.[24] Air-liquid interface NCI-H441 cells may provide a useful model system to study this aspect of paracellular permeability using genetic modification or chemical perturbation to modulate the expression and function of specific claudins.[7]

ACKNOWLEDGMENTS

Author VS declares that he has no conflict of interest. This work was supported by the RSNZ Marsden Fund (Grant No. UOA-1411).

REFERENCES

[1]Beck, R. E., and J. S. Schultz. Hindrance of solute diffusion within membranes as measured with microporous membranes of known pore geometry. *Biochim. Biophys. Acta*. 255:273–280, 1972.
[2]Cipolla, D. Will pulmonary drug delivery for systemic application ever fulfill its rich promise. *Expert Opin. Drug Deliv*. 13(10):1337–1340, 2016.
[3]Cryan, S. A., N. Sivadas, and L. Garcia-Contreras. In vivo animal models for drug delivery across the lung mucosal barrier. *Adv. Drug. Deliv. Rev*. 59:1133–1151, 2007.
[4]Ehrhardt, C., J. Fiegel, S. Fuchs, R. Abu-Dahab, U. F. Schaefer, J. Hanes, and C. M. Lehr. Drug absorption by the respiratory mucosa: cell culture models and particulate drug carriers. *J. Aerosol. Med*. 15:131–139, 2002.
[5]Ehrhardt, C., K.-J. Kim, and M. Laue. In Vitro Models of the Alveolar Epithelial Barrier Drug Absorption Studies. New York: Springer, pp. 258–282, 2008.
[6]Elbert, K. J., U. F. Schafer, H. J. Schafers, K. J. Kim, V. H. L. Lee, and C. M. Lehr. Monolayers of human alveolar epithelial cells in primary culture for pulmonary absorption and transport studies. *Pharm. Res*. 16:601–608, 1999.
[7]Frank, J. A. Claudins and alveolar epithelial barrier function in the lung. *Ann. N. Y. Acad. Sci*. 1257:175–183, 2012.
[8]Frost, T. S., L. Jiang, R. M. Lynch, and Y. Zohar. Permeability of epithelial/endothelial barriers in transwells and microfluidic bilayer devices. *Micromachines*. 10:533, 2019.
[9]Ghadiri, M., P. M. Young, and D. Traini. Strategies to enhance drug absorption via nasal and pulmonary routes. *Pharmaceutics*. 11(13):113, 2019.
[10]Günzel, D., and A. D. Yu. Claudins and the modulation of tight junction permeability. *Physiol. Rev*. 93(2):525–569, 2013.
[11]Huh, D., B. D. Matthews, A. Mammoto, M. Montoya-Zavala, H. Y. Hsin, and D. E. Ingber. Reconstituting organ-level lung functions on a chip. *Science*. 328:1662–1668, 2010.
[12]Kim, K. J., Z. Borok, and E. D. Crandall. A useful in vitro model for transport studies of alveolar epithelial barrier. *Pharm. Res*. 18:253–255, 2001.
[13]Kobayashi, S., S. Kondo, and K. Juni. Permeability of peptides and proteins in human cultured alveolar A549 cell monolayer. *Pharm. Res*. 12:1115–1119, 1995.

[14]Matsukawa, Y., V. H. L. Lee, E. D. Crandall, and K. J. Kim. Size dependent dextran transport across rat alveolar epithelial cell monolayers. *J. Pharm. Sci.* 86:305–309, 1997.
[15]Nalayanda, D. D., C. Puleo, W. B. Fulton, L. M. Sharp, T.-H. Wang, and F. Abdullah. An open-access microfluidic model for lung-specific functional studies at an air-liquid interface. *Biomed. Microdevices.* 11:1081, 2009.
[16]Overgaard, C. E., L. A. Mitchell, and M. Koval. Roles for claudins in alveolar epithelial barrier function. *Ann. N. Y. Acad. Sci.* 1257(1):167–174, 2012.
[17]Patton, J. S., C. S. Fishburn, and J. G. Weers. The lungs as a portal of entry for systemic drug delivery. *Proc. Am. Thorac. Soc.* 1(4):338–344, 2004.
[18]Ren, H., N. P. Birch, and V. Suresh. An optimised human cell culture model for alveolar epithelial transport. *PLoS ONE.* 11:e0165225, 2016.
[19]Sakagami, M. In vivo, in vitro and ex vivo models to assess pulmonary absorption and disposition of inhaled therapeutics for systemic delivery. *Adv. Drug Deliv. Rev.* 58:1030–1060, 2006.
[20]Salomon, J. J., V. E. Muchitsch, J. C. Gausterer, E. Schwagerus, H. Huwer, N. Daum, C. M. Lehr, and C. Ehrhardt. The cell line NCl-H441 is a useful in vitro model for transport studies of human distal lung epithelial barrier. *Mol. Pharm.* 11(3):995–1006, 2014.
[21]Stucki, J. D., N. Hobi, A. Galimov, et al. Medium throughput breathing human primary cell alveolus-on-chip model. *Sci. Rep.* 8:14359, 2018.
[22]Watson, C. J., M. Rowland, and G. Warhurst. Functional modeling of tight junctions in intestinal cell monolayers using polyethylene glycol oligomers. *Am. J. Physiol. Cell Physiol.* 281:C388-397, 2001.
[23]Zamprogno, P., S. Wüthrich, S. Achenbach, et al. Second-generation lung-on-a-chip with an array of stretchable alveoli made with a biological membrane. *Commun. Biol.* 4:168, 2021.
[24]Zihni, C., C. Mills, K. Matter, et al. Tight junctions: from simple barriers to multifunctional molecular gates. *Nat. Rev. Mol. Cell Biol.* 17:564–580, 2016.